Dynamics of a nonconserving Davydov monomer

P. A. S. Silva and L. Cruzeiro*
CCMAR and FCT, University of Algarve, Campus de Gambelas, 8000 Faro, Portugal
(Received 7 December 2005; revised manuscript received 5 May 2006; published 28 August 2006)

The Davydov-Scott model describes the transfer of energy along hydrogen-bonded chains, like those that stabilize the structure of α helices. It is based on the hypothesis that amide I excitations are created (by the hydrolysis of ATP, for instance) and kept in the system. Recent experimental results confirm that the energy associated with amide I excitations does indeed last for tens of picoseconds in proteins and model systems. However, the Davydov-Scott model cannot describe the conversion of that energy into work, because it conserves the number of excitations. With the aim of describing conformational changes, we consider, in this paper, a nonconserving generalization of the model, which is found to describe essentially a contraction of the hydrogen bond adjacent to the site where an excitation is present. Unlike the one-site Davydov-Scott model, that contraction is time dependent because the number of excitations is not conserved. However, considering the time average of the dynamical variables, the results reported here tend to the known results of the Davydov-Scott model.

DOI: 10.1103/PhysRevE.74.021920 PACS number(s): 87.15.He, 87.10.+e, 87.15.Aa

I. INTRODUCTION

It has been known for a long time that most functions performed by proteins in living cells are driven by the hydrolysis of adenosine triphosphate (ATP). This step provides the necessary energy for the task performed by a protein, which usually involves conformational changes. The detailed mechanism for the conversion of the chemical energy released in ATP hydrolysis into work is still unknown.

In the 1970s McClare [1] suggested that the energy released in the hydrolysis of ATP could be stored in the form of a vibrational excited state of some group in the polypeptide chain. The presence of similar groups at neighboring points in the chain would allow a resonant exchange of energy between them. The main point of this hypothesis was that vibrational excited states should have a long enough lifetime in the protein (before they decay into heat or lead to emission) in order to become useful for work. McClare argued that proteins evolved in such a way as to promote the enhancement of those lifetimes.

These ideas underwent further development with the work of Davydov [2,3]. According to Davydov, the hydrolysis of ATP produces vibrational excited states at the active site of the protein in the form of amide I excitations, which correspond essentially to a stretching of the C═O bond in a peptide group. The aim of the theory developed by Davydov was to describe the collective excitations of linear chains consisting of peptide groups connected by hydrogen bonds (like the ones that stabilize α helices). His model predicts a localized ground state for the collective excitation with an energy lower than that of its free state [2]. In the ground state the excitation has the possibility of traveling along the chain with a group velocity proportional to the energy of the interaction between peptide groups. It is also predicted that the presence of an amide I excitation in a given peptide group produces a contraction of the adjacent hydrogen bond. As the excitation moves along the chain, so does the associated distortion. This traveling ground state, consisting of an amide I excitation together with the associated distortion, is the so-called Davydov soliton. The excitation is localized by the distortion it itself induced, a phenomenon called self-trapping. It was argued that the soliton has a longer lifetime than the isolated amide I excitation [4] in accordance with the needs of a molecular machine, as pointed out by McClare [1].

Davydov's theory was initially developed for a $\Theta=0$ K system. A large amount of work has been done on the properties of Davydov's soliton [4], including some generalizations to biological temperatures. It has been shown [5] that, at these temperatures, the localization of the amide I excitation is conserved but it is no longer correlated with an induced lattice distortion. At biological temperatures, the amide I excitations are localized, not by self-trapping, but by static and dynamic disorder, and the soliton becomes a very improbable state. However, the localized excitation is able to travel in a Brownian-like motion along the chain, driven by thermal vibrations. In this way it can be transferred from one site to a distant region of the chain in a few picoseconds.

These results suggest that, although the coherent transfer of energy is lost at biological temperatures, there is still a mechanism, based on Davydov's model, which can provide an explanation for the transport of energy in proteins.

The first experimental evidence of a self-trapped state was found in acetanilide by Careri and co-workers [6]. Acetanilide is an organic crystal which is used very often as a model for polypeptides because bond distances and angles are similar in both kinds of system. The existence of that state was confirmed by Edler and Hamm [7,8] in acetanilide and *N*-methylacetamide [9]. Their work on acetanilide showed that, at low temperatures, the so-called anomalous amide I band (1650 cm^{-1}) can be assigned to a self-trapped state, while the normal amide I band (1666 cm^{-1}) corresponds to a

*Electronic adress: lhansson@ualg.pt

delocalized state. With increasing temperature the self-trapped state is destroyed and thermal disorder localizes the 1666 cm^{-1} band. If both the 1650 and the 1666 cm^{-1} states are excited at 90 K, the energy is kept in the crystal for 35 ps before it reappears in the form of heat [7]. The measured relaxation is faster at room temperature (12 ps). When compared with the relaxation time measured for the amide I band of acetanilide molecules dissolved in isopropyl alcohol (1 ps) [7], those relaxation times show that the crystalline structure is essential to delay the dissipation of the excitation energy, as previously suggested.

Austin and co-workers, on the other hand, measured the properties of the amide I band in myoglobin [10]. They found a temperature-dependent peak at 1626 cm^{-1} which disappears as the temperature rises, and another one, at 1661 cm^{-1}, that is essentially temperature-independent. The low-lying state was identified as a self-trapped state. While no significant differences are found in the relaxation times for excitations of 1626 and 1661 cm^{-1} at 280 K, this is not the case at 50 K. Indeed, at this low temperature the excitations have very distinct lifetimes: 30 ps for the 1626 cm^{-1} one, six times larger than the 5 ps lifetime of the 1661 cm^{-1} excitation.

The experimental results mentioned, together with the theoretical work, do indicate that the H-bonded spines promote the capability of storing energy in proteins and model systems alike. Still missing is an understanding of how proteins can use the energy stored in this manner to undergo conformational changes [11].

In this paper we are concerned with a generalized Davydov-Scott model that may eventually explain conformational changes. This model is not conservative in the number of excitations in the system. The idea is that the decay of an excitation can release the necessary energy for the protein to undergo a conformational change. In Sec. II the Hamiltonian of the system is presented and the equations of motion ($\Theta=0$ K) are derived. Numerical solutions for these equations are presented and discussed in Sec. III. In Sec. IV adiabatic and "quasistatic" approximations are performed on the equations of motion. The analytical results from these approximations are compared with the numerical results. Finally, some conclusions are given in Sec. V.

II. THE EQUATIONS OF MOTION

Davydov's Hamiltonian describes the dynamics of amide I excitations traveling along the chains of hydrogen bonds that stabilize α helices. Such chains can be idealized as follows:

$$\cdots \mathrm{H}-\underset{(n-1)}{\mathrm{N}}-\mathrm{C}=\mathrm{O}\cdots\mathrm{H}-\underset{(n)}{\mathrm{N}}-\mathrm{C}=\mathrm{O}\cdots\mathrm{H}-\underset{(n+1)}{\mathrm{N}}-\mathrm{C}=\mathrm{O}\cdots .$$

The Hamiltonian for this system assumes the form [4]

$$\hat{H}=\hat{H}_{ex}+\hat{H}_{int}+\hat{H}_{ph}, \tag{1}$$

with

$$\hat{H}_{ex}=\sum_n\left[\varepsilon_0\left(\hat{a}_n^\dagger\hat{a}_n+\frac{1}{2}\right)-J(\hat{a}_n^\dagger\hat{a}_{n+1}+\hat{a}_n^\dagger\hat{a}_{n-1})\right], \tag{2}$$

$$\hat{H}_{ph}=\frac{1}{2}\sum_n\left(\frac{\hat{p}_n^2}{M}+k(\hat{u}_{n+1}-\hat{u}_n)^2\right), \tag{3}$$

$$\hat{H}_{int}=\chi\sum_n\left[(\hat{u}_{n+1}-\hat{u}_n)\left(\hat{a}_n^\dagger\hat{a}_n+\frac{1}{2}\right)\right]. \tag{4}$$

In Eq. (1) $\hat{H}_{ex}$ is the excitation Hamiltonian, describing the states of the amide I excitation, which correspond essentially to a stretching of the C=O bond. $\hat{H}_{ph}$ is the phonon Hamiltonian, which describes the vibrations of the chain of amino acids mediated by the hydrogen bonds. $\hat{H}_{int}$ describes the interaction of the excitations with the lattice vibrations. In Eqs. (2) and (4) $\hat{a}_n^\dagger$ and $\hat{a}_n$ are the boson creation and annihilation operators for amide I excitations at the site n of the chain; $\hat{u}_n$ is the (quantum) displacement of site n from its equilibrium position and $\hat{p}_n$ is the (quantum) momentum of site n. The sums are considered over all sites in the chain. The parameters of the theory are ε_0, the energy of an isolated amide I vibration; $-J$, which is the nearest-neighbor dipole-dipole coupling along the chain; M is the mass of an amino acid, considered to be the same at all sites; k stands for the elasticity constant of the lattice; and χ is the excitation-phonon coupling parameter.

The operator that gives the total number of excitations in the system ($\hat{N}=\Sigma_n\hat{a}_n^\dagger\hat{a}_n$) commutes with the Hamiltonian (2), (3), and (4). For this reason the total number of excitations is conserved in the dynamics of the system. Our objective in this paper is to generalize Hamiltonian (2) in order to allow the creation and annihilation of amide I excitations. Since the total energy of the system is also a constant of the movement ($\hat{H}$ commutes with itself), it is expected that the energy released by the decay of an amide I quantum will eventually have some effect in the lattice vibrations. In this way, we aim at developing a model that can explain how the energy stored in the amide I vibrations can be used to generate conformational changes. Because the effective number of degrees of freedom increases very fast with the number of sites, here we address this problem in a simplified manner and consider a small lattice of just two sites where only one of them is able

to support amide I vibrations. Such a system can be idealized as follows:

$$\mathrm{H}-\mathrm{N}-\mathrm{C}=0\cdots\mathrm{H}-\mathrm{N}-\mathrm{C}-R.$$

In this lattice, amide I excitations can exist only in the first site. —R stands for some radical bonded to the right-hand site and the sites are hydrogen bonded to each other. This simplified system does not allow for the transfer of excitations between sites. If an amide I quantum is present, at some time instant, in the system, it may either stay there or decay, releasing its rest energy. A more general system will have to deal with a competition between the decay of a quantum and its transfer to another site. Our main goal here is to model the nonconservation of amide I excitations. The general case will be an extension of the present one.

The Hamiltonian for this system can be written as in (1) but with the terms

$$\hat{H}_{ex} = \varepsilon_0\left(\hat{a}^\dagger\hat{a} + \frac{1}{2}\right), \tag{5}$$

$$\hat{H}_{ph} = \frac{1}{2}\left(\frac{\hat{p}^2}{M} + k\hat{u}^2\right), \tag{6}$$

$$\hat{H}_{int} = \chi\hat{u}\left(\hat{a}^\dagger\hat{a} + \frac{1}{2}\right), \tag{7}$$

where the symbols have the same meaning as in Eqs. (2), (3), and (4) with the exceptions of M, which, in Eq. (6), symbolizes the reduced mass of the two sites, $\hat{u}$, which represents the elongation of the hydrogen bond relative to its equilibrium length, and $\hat{p}$, which is the relative momentum.

In order to be able to describe conformational changes, we propose to write the excitation Hamiltonian $\hat{H}_{ex}$ in the form

$$\hat{H}_{ex}^{nc} = \varepsilon_0\left(\hat{a}^\dagger\hat{a} + \frac{1}{2}\right) + T(\hat{a}^\dagger + \hat{a}), \tag{8}$$

where T is a new parameter, related to the variation of the number of amide I quanta, and the superscript nc stands for nonconserved amide I number. This extra term can be interpreted as the interaction of a dipole with an *internal* electric field, but its role here is to break the conservation of amide I number. Indeed, for conformational changes to occur, the energy stored in the amide I excitation must be made available to the lattice degrees of freedom. In this context, T represents the strength of the *intramolecular* interactions that may cause the release of the amide I energy.

We will therefore be studying in this paper the Hamiltonian

$$\hat{H}^{nc} = \hat{H}_{ex}^{nc} + \hat{H}_{int} + \hat{H}_{ph}, \tag{9}$$

where the three terms in Eq. (9) are given by Eqs. (6), (7), and (8).

Let us consider $|\Psi(t)\rangle$ as a generic state of the system. We are interested in the time evolution of the quantum averages of a number of dynamical variables, like the number of amide I excitations and the stretching of the lattice. Using Ehrenfest's theorem one obtains

$$\frac{d\langle\hat{n}\rangle}{dt} = -\frac{i}{\hbar}\langle[\hat{n},\hat{H}^{nc}]\rangle = -\frac{i}{\hbar}\langle[\hat{a}^\dagger\hat{a},\hat{H}^{nc}]\rangle = -\frac{i}{\hbar}T\langle\hat{a}^\dagger\rangle + \frac{i}{\hbar}T\langle\hat{a}\rangle, \tag{10}$$

where $\langle\hat{O}\rangle$ denotes $\langle\Psi(t)|\hat{O}|\Psi(t)\rangle$. Setting $n(t)=\langle\hat{n}\rangle$ and $\xi(t)=\langle\hat{a}\rangle$, Eq. (10) can be rewritten in the form

$$\dot{n}(t) = \frac{i}{\hbar}T[\xi(t) - \xi^*(t)]. \tag{11}$$

In the same way, the time evolution for the mean value of the displacement operator can be written as

$$\frac{d\langle\hat{u}\rangle}{dt} = -\frac{i}{\hbar}\langle[\hat{u},\hat{H}^{nc}]\rangle = \frac{\langle\hat{p}\rangle}{M}, \tag{12}$$

or, defining $u(t)=\langle\hat{u}\rangle$ and $p(t)=\langle\hat{p}\rangle$,

$$\dot{u}(t) = \frac{p(t)}{M}. \tag{13}$$

In order to have a complete set of equations for the dynamical variables of the system, the time evolution of $\xi(t)$ and $p(t)$ must be found. The use of Ehrenfest's theorem gives

$$\dot{\xi}(t) = \frac{d\langle\hat{a}\rangle}{dt} = -\frac{i}{\hbar}\langle[\hat{a},\hat{H}^{nc}]\rangle = -\frac{i}{\hbar}\langle(\varepsilon_0 + \chi\hat{u})\hat{a}\rangle - \frac{i}{\hbar}T \tag{14}$$

and

$$\dot{p}(t) = \frac{d\langle\hat{p}\rangle}{dt} = -\frac{i}{\hbar}\langle[\hat{p},\hat{H}^{nc}]\rangle = -\chi\left(n(t) + \frac{1}{2}\right) - ku(t). \tag{15}$$

Equations (11), (13), (14), and (15) constitute a complete set of differential equations for the mean values of the relevant operators of the system. All operators appear uncorrelated in this set of equations with the exception of $\hat{u}$ and $\hat{a}$ in Eq. (14).

This set of equations is similar to the reduced set of equations (RSE) published elsewhere [12]. These latter equations were derived assuming, from the beginning, that the variables related to the lattice dynamics are classical [real numbers $u(t)$ and $p(t)$ are used instead of the operators $\hat{u}$ and $\hat{p}$]. The justification for this assumption lies in the fact that the masses of the lattice sites are big enough to allow the quantum fluctuations of the lattice operators to be neglected.

In this paper we adopt a full quantum description and Eq. (14) shows that the RSE is recovered if the correlations between $\hat{u}$ and $\hat{a}$ are neglected. This approximation is

less restrictive than assuming classical dynamics for the lattice. When the correlations between $\hat{u}$ and $\hat{a}$ are neglected, Eq. (14) can be written as in (16) and, in that case, Eqs. (11), (13), (15), and (16) become formally identical to the RSE:

$$\dot{\xi}(t) = -\frac{i}{\hbar}[\varepsilon_0 + \chi u(t)]\xi(t) - \frac{i}{\hbar}T. \tag{16}$$

We should note that these equations are valid (within the approximations assumed) for $\Theta = 0$ K. It has been shown [13] that, although there are some differences in the behaviors of the semiclassical and the full quantum systems at low temperatures, their thermal equilibrium properties are indistinguishable above ≈ 11 K. This result indicates that the quantum fluctuations of the lattice operators are small when compared with their thermal fluctuations above that temperature. In this paper we do not consider the effects of temperature. Thus, since Eqs. (11), (13), (15), and (16) are the same as those obtained in the semiclassical approximation, it is expected that the details of the dynamics will differ from the results that would be obtained for the full quantum system.

III. NUMERICAL SOLUTIONS

Considering the real and imaginary parts of the complex variable $\xi(t) = \xi_r(t) + i\xi_i(t)$, the equations of motion can be written, using only real functions of the time, in the form

$$\dot{n}(t) = -\frac{2T}{\hbar}\xi_i(t), \tag{17}$$

$$\xi_r(t) = \frac{\varepsilon_0 + \chi u(t)}{\hbar}\xi_i(t), \tag{18}$$

$$\xi_i(t) = -\frac{\varepsilon_0 + \chi u(t)}{\hbar}\xi_r(t) - \frac{T}{\hbar}, \tag{19}$$

$$\dot{u}(t) = \frac{p(t)}{M}, \tag{20}$$

$$\dot{p}(t) = -\chi\left(n(t) + \frac{1}{2}\right) - ku(t). \tag{21}$$

Equations (17)–(21) have been numerically integrated taking the parameters to be the same as for the Davydov-Scott model [4] ($\varepsilon_0 = 1660$ cm^{-1}, $\chi = 62$ pN, $k = 13$ N m^{-1}, and $M = 114$ amu). The system was started with one or two amide I excitations because the energy released in the process of ATP hydrolysis is not enough to create initial states with more excitations. For the remaining variables the assignment of initial conditions is not as well defined. For this reason, a number of sets of initial conditions were considered. A simulation time of 100 ps was considered to be a good reference since, as pointed out before, the relevant features of the dynamics should occur in tens of picoseconds. The quality of these numerical solutions was continuously verified by observing the conservation of the total energy and

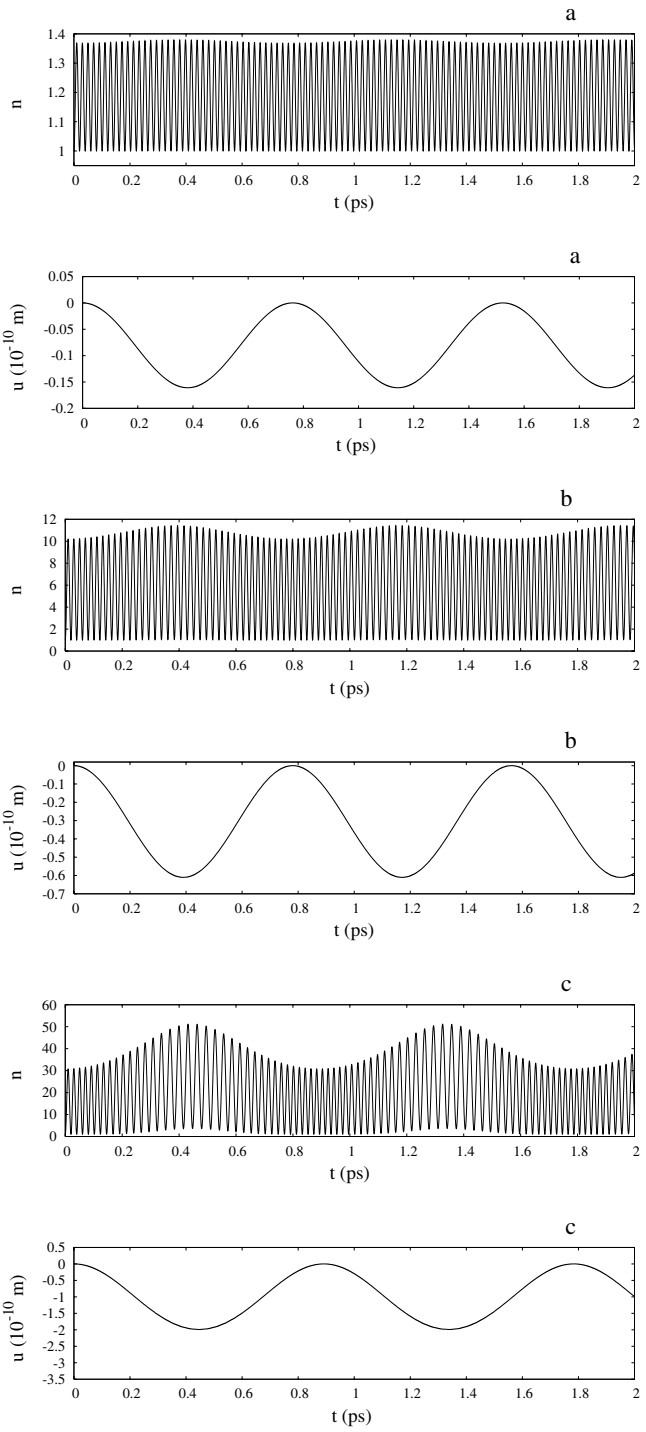

FIG. 1. Numerical solutions of Eqs. (17)–(21). The results displayed are for the average number of excitations (n) and the lattice distortion (u) with T=(a) 10, (b) 50, and (c) 90 (in units of 10^{-21} J). Only the first 2 ps of a 100 ps simulation are shown. The initial conditions are $\xi_{r0} = \xi_{i0} = 0$, $u_0 = 0$ (10^{-10} m), $p_0 = 0$ (10^{-23} kg m s^{-1}), and $n_0 = 1$.

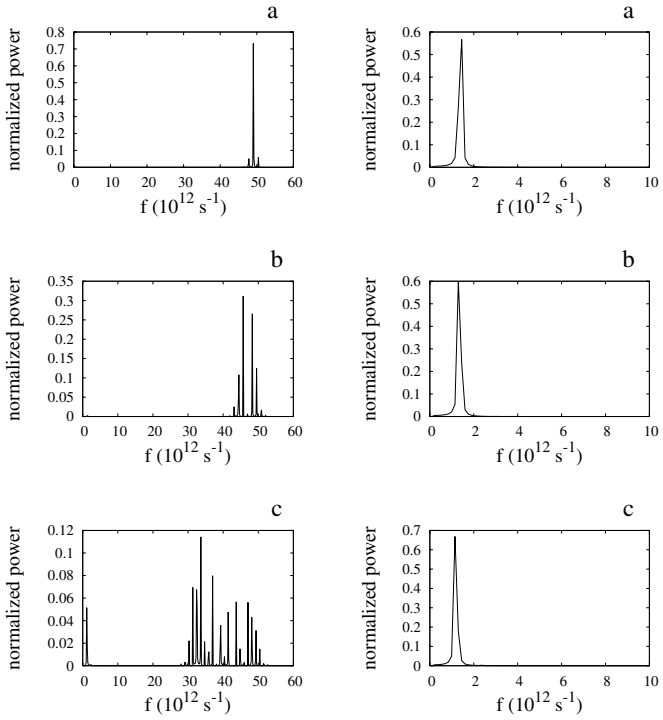

FIG. 2. Spectra obtained from the numerical solutions displayed in Fig. 1. The plots on the left side are the Fourier transforms of the average number of excitations while those on the right side are the Fourier transforms of the lattice distortion. The values of the parameter T are (a) 10, (b) 50, and (c) 90 (in units of 10^{-21} J).

by checking the quantity $n(t)-|\xi(t)|^2$, which is also conserved by Eqs. (17)–(21) [12].

The dynamics described by Eqs. (17)–(21) was explored for values of the unknown parameter T ranging from 1 to 100 (10^{-21} J). The conservation of the previously mentioned quantities was verified to nine significant digits throughout the entire simulation time, i.e., for 100 ps, for all T values below 99.7. For $T=99.7$ and $T=100$ some fluctuations arose after ≈ 2 ps. These fluctuations never affected more than the last three or four digits within the simulation time.

The reasons for stopping at $T=100$ are twofold: the less precise conservation of the energy [and of $n(t)-|\xi(t)|^2$] for T greater than this value, on the one hand, and the physical limits for the lattice contraction, on the other. The first reason is related to a decrease in the performance of the integrator in the regimes of large T values. The second comes from the characteristics of typical α helices. In fact, the known values for the C-N average distances of hydrogen bonds associated with α helices are ≈ 3 Å. The lattice distortion reaches such values for $T>99.69$. For this reason, larger values of T lead to unrealistic results.

Figure 1 shows the results obtained for the average number of excitations $n(t)$ as well as for the lattice distortion $u(t)$ for three representative values of T. The initial conditions for this simulation are $\xi_{r0}=\xi_{i0}=0$, $u_0=0$ (10^{-10} m), $p_0=0$ (10^{-23} kg m s^{-1}), and $n_0=1$.

A general feature of the results obtained for different T values is that $n(t)$ is not constant, as it would be for the Davydov-Scott model, and instead it shows a rapid

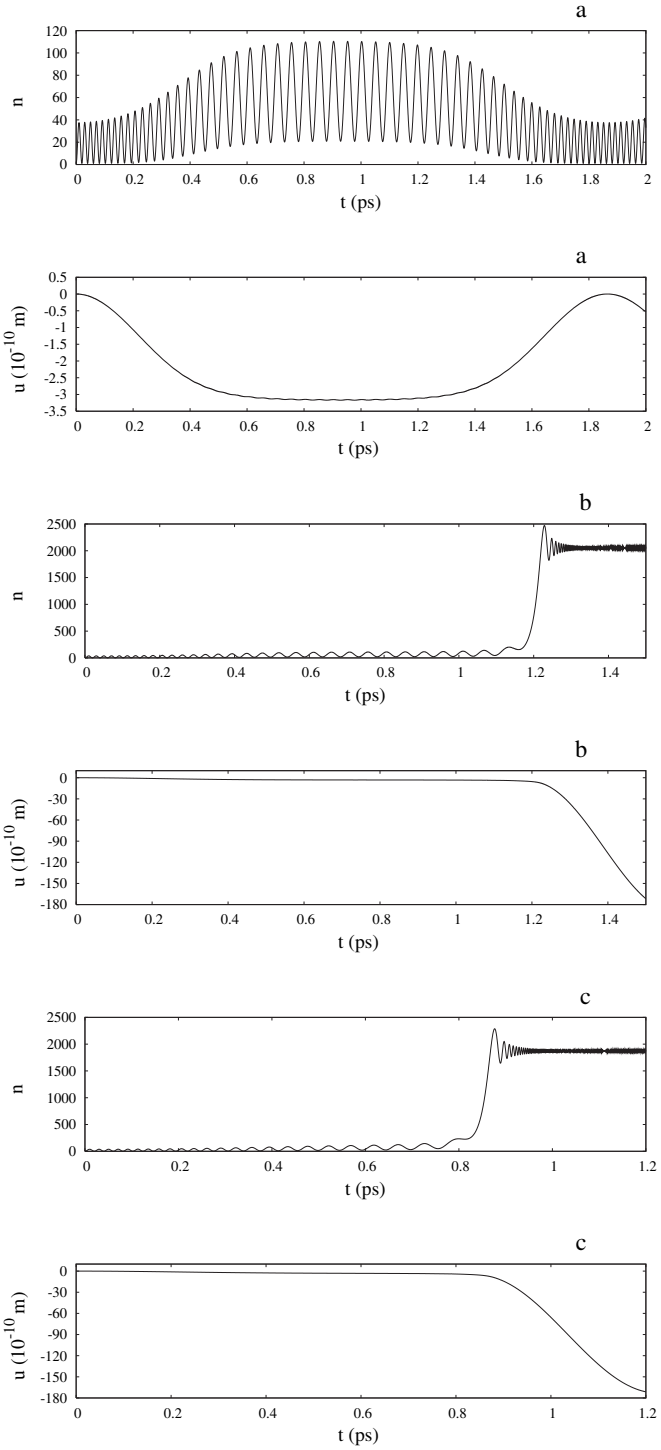

FIG. 3. Average number of excitations (n) and lattice distortion (u) for $T=$(a) 99.69, (b) 99.7, and (c) 100 (in units of 10^{-21} J). Only the first part of a 100 ps simulation is shown. The initial conditions are as in Fig. 1. The conservation of the quantities mentioned in the text is observed for the entire time range displayed.

oscillation modulated by a slower frequency, while $u(t)$ behaves approximately like an oscillator driven by an effective force related to the time average of $n(t)$. The change in the dynamics of the system with T is also apparent in Fig. 1. The

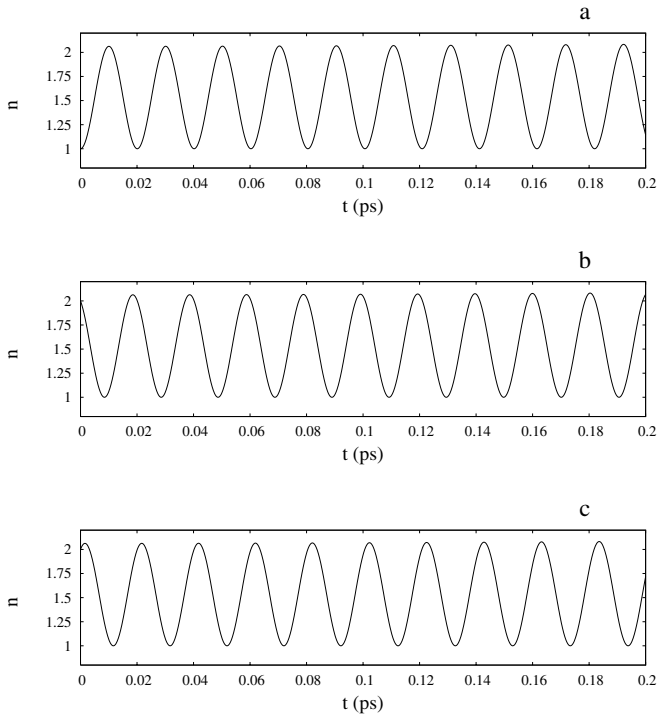

FIG. 4. Average number of excitations for $T=17$ (in units of 10^{-21} J). The initial conditions are (a) $\xi_{r0}=\xi_{i0}=0$, $u_0=0$ (10^{-10} m), $p_0=0$ (10^{-23} kg m s^{-1}), and $n_0=1$; (b) $\xi_{r0}=-\varepsilon_0/2T$, $\xi_{i0}=\sqrt{1-\xi_{r0}^2}$, $u_0=0$ (10^{-10} m), $p_0=0$ (10^{-23} kg m s^{-1}), and $n_0=2$; (c) $\xi_{r0}=-\varepsilon_0/2T$, $\xi_{i0}=-\sqrt{1-\xi_{r0}^2}$, $u_0=0$ (10^{-10} m), $p_0=0$ (10^{-23} kg m s^{-1}), and $n_0=2$. All cases correspond to the same total energy and the same value of $\langle n\rangle-|\xi|^2$.

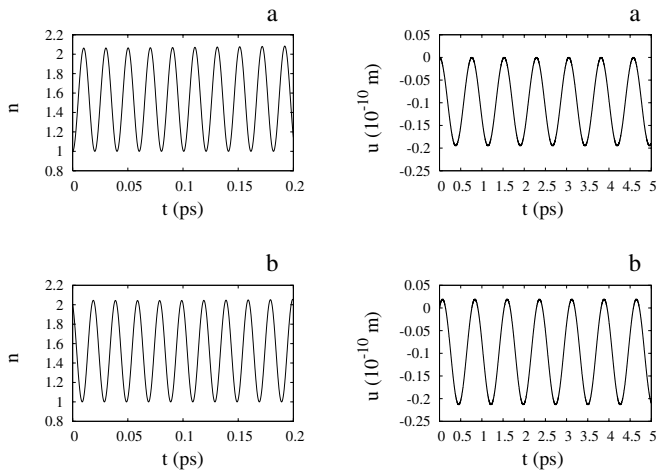

FIG. 5. Average number of excitations (n) and lattice distortion (u) for $T=17$ (in units of 10^{-21} J). The initial conditions are (a) $\xi_{r0}=\xi_{i0}=0$, $u_0=0$ (10^{-10} m), $p_0=0$ (10^{-23} kg m s^{-1}), and $n_0=1$; (b) $\xi_{r0}=-\varepsilon_0/2T-1/4TM$, $\xi_{i0}=\sqrt{1-\xi_{r0}^2}$, $u_0=0$ (10^{-10} m), $p_0=1$ (10^{-23} kg m s^{-1}), and $n_0=2$. All cases correspond to the same total energy and the same value of $\langle n\rangle-|\xi|^2$.

baseline level of $n(t)$ $[u(t)]$ is found to increase (decrease) with T following a law that can be fitted to a third-order polynomial function. An evident feature of the system is the correlation between the dynamics of the lattice distortion and the modulation of $n(t)$.

In the regime of small T the modulation is very weak and the oscillation of $n(t)$ occurs at a constant frequency during the entire simulation time. This observation is confirmed by the Fourier transform of $n(t)$ which shows essentially a strong single peak at the frequency $f\approx\varepsilon_0/2\pi\hbar$ (see Fig. 2). As T is increased, the spectrum of $n(t)$ becomes more and more complex around this frequency. The general trend for the evolution of the spectra with T is the appearance of more and more frequencies below $f\approx\varepsilon_0/2\pi\hbar$ as T is increased, while a peak at very low frequency $[f\approx(1/2\pi)\sqrt{k/M}]$ grows stronger. This last frequency turns out to be the single frequency of oscillation of $u(t)$, which is essentially kept for all regimes of T (Fig. 2). For $T=90$ [Fig. 1(c)] these features are easily observable: the variation of the frequency of rapid oscillation is apparent as well as the strong modulation in amplitude with the frequency of the lattice oscillation.

As described above, Fig. 1 suggests that the dynamics of the system varies continuously with T. However, this is so up to a certain value of T (T_c), above which there occurs a sudden change in the time evolution of $n(t)$ and $u(t)$. Figure 3 displays the results for $T=99.69$, 99.7, and 100 (10^{-21} J).

$T_c=99.69$ defines a separation between two qualitatively very distinct dynamical regimes. As mentioned above, only the cases with $T<99.69$ may be considered to have physical relevance. For $T>99.69$ the system attains a high average number of excitations and the lattice is driven to a physically impossible contraction.

Equations (17)–(21) were solved for initial conditions different from those that have been studied above, but corresponding to the same values of energy and $n(t)-|\xi(t)|^2$. The differences between these other solutions and the cases previously discussed are observed mainly in the phase of the oscillations. Figure 4 shows the typical behavior observed for sets of initial conditions that include $u_0=0$ (10^{-10} m) and $p_0=0$ (10^{-23} kg m s^{-1}). In these cases the phases of $n(t)$ are very distinct while the dynamics is essentially the same. No differences are observed in the behavior of $u(t)$ for the various sets of initial conditions tried. Moreover, Figs. 4(b) and 4(c) show an interesting result: although the corresponding simulations differ only in the phase of the complex initial parameter ξ_0, the results are nevertheless distinct. This is not usually expected in quantum systems since only real parameters, that is, the absolute values of physical variables, are measurable and therefore meaningful, but it is known to happen in nonlinear systems [14].

For the results in Fig. 5 the initial energy in the lattice degrees of freedom was not zero (while the total energy of the system was kept as in previous cases). Comparing Figs. 5(a) and 5(b) the previously mentioned difference in phase is apparent [this time both in $n(t)$ and in $u(t)$] and, more physically significantly, the amplitudes of both functions are also different. The amplitude of $u(t)$ is enhanced in the case of Fig. 5(b), while a small decrease in the amplitude of $n(t)$ occurs.

The overall conclusion is that, for $T<99.69$ (10^{-21} J), the dynamical regimes are not strongly dependent on the initial conditions, i.e., the solutions found evolve in time in a similar way. The general behavior described in association with Fig. 1 can thus be generalized for different initial conditions (as long as T is within the values for which the dynamical variables of the system are kept physically meaningful).

IV. THE QUASISTATIC APPROXIMATION

From the numerical results shown, the occurrence of (at least) two very different time scales in the dynamics of the system is clear. In the regimes considered physically relevant, the oscillation of the average number of excitations is much faster than the movement associated with the lattice (see for instance Fig. 1). This is not surprising since the last one involves the dislocation of massive sites. For this reason a tentative interpretation of the previous results in terms of an adiabatic approximation was performed. This approximation consists in considering a motion of the lattice that is much slower than the reaction of the excitation dynamics.

Mathematically we have

$$\dot{p}(t) \approx 0. \tag{22}$$

Using this condition in Eqs. (17)–(21) gives (see the Appendix)

$$\ddot{n}(t) = -\alpha n^3(t) + \beta n^2(t) - \gamma(n_0, \xi_{r0}) n(t) + \delta(n_0, \xi_{r0}) + \frac{2T^2}{\hbar^2}, \tag{23}$$

where α, β, γ, and δ are the parameters of the equation, depending on the initial conditions as well as on the parameters of the Hamiltonian.

Making use of the auxiliary function $y=\dot{n}$, one may write Eq. (23) in the form

$$\ddot{n} = \dot{y} = \frac{dy}{dn}\dot{n} = y\frac{dy}{dn} = -\alpha n^3 + \beta n^2 - \gamma n + \delta + \frac{2T^2}{\hbar^2},$$

and integrating the last equality gives

$$y^2 \equiv \left(\frac{dn}{dt}\right)^2 = -\frac{\alpha}{2}(n^4 - n_0^4) + \frac{2}{3}\beta(n^3 - n_0^3) - \gamma(n^2 - n_0^2) + 2\left(\delta + \frac{2T^2}{\hbar^2}\right)(n - n_0) + \frac{4T^2}{\hbar^2}\xi_{i0}^2. \tag{24}$$

Equations like (24) have been found before in connection with the problem of finding traveling-wave solutions for the equations of motion, in the context of the conservative Davydov-Scott Hamiltonian [15]. In the present case, the solutions of Eq. (24) describe the dynamics associated with the number of excitations in the adiabatic approximation. Those solutions are qualitatively different depending on the shape of the quartic polynomial shown on the right hand side of the equation. Its shape is, in turn, modeled by the unknown parameter T. The different types of solutions will thus be labeled by the values of T.

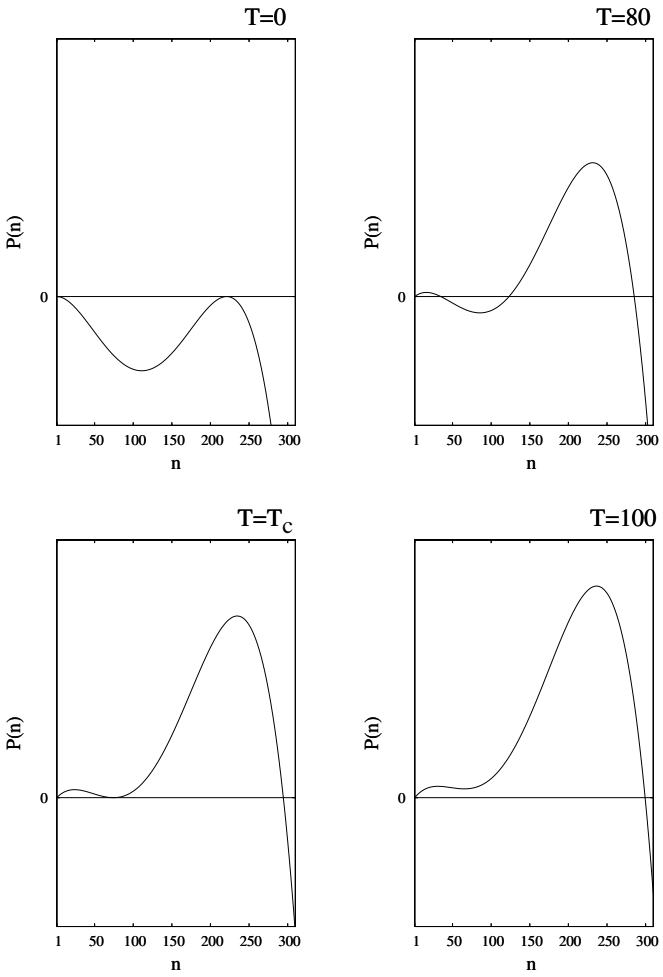

FIG. 6. Different forms of the quartic polynomial in Eq. (25) as functions of T. The different regimes found are $T=0$, $0<T<T_c$, $T=T_c$, and $T>T_c$.

Considering the initial conditions in Figs. 1 and 3, Eq. (24) assumes the form

$$y^2 \equiv \left(\frac{dn}{dt}\right)^2 = -\frac{\alpha}{2}(n^4 - 1) + \frac{2}{3}\beta(n^3 - 1) - \gamma(n^2 - 1) + 2\left(\delta + \frac{2T^2}{\hbar^2}\right)(n - 1). \tag{25}$$

In this form, the parameters of the polynomial depend only on the second power of T and, for this reason, its sign is not relevant for the dynamics of the excitations. Therefore, from this point on we will be concerned with what happens for positive values of T.

There are four different possibilities for the polynomial in Eq. (25), which are displayed in Fig. 6. The corresponding regimes of Eq. (25) are associated with the following values of T: $T=0$, $0<T<T_c$, $T=T_c$, and $T>T_c$, where $T_c=\sqrt{(2k/3^3\chi^2)(\varepsilon_0-3\chi^2/2k)^3}$.

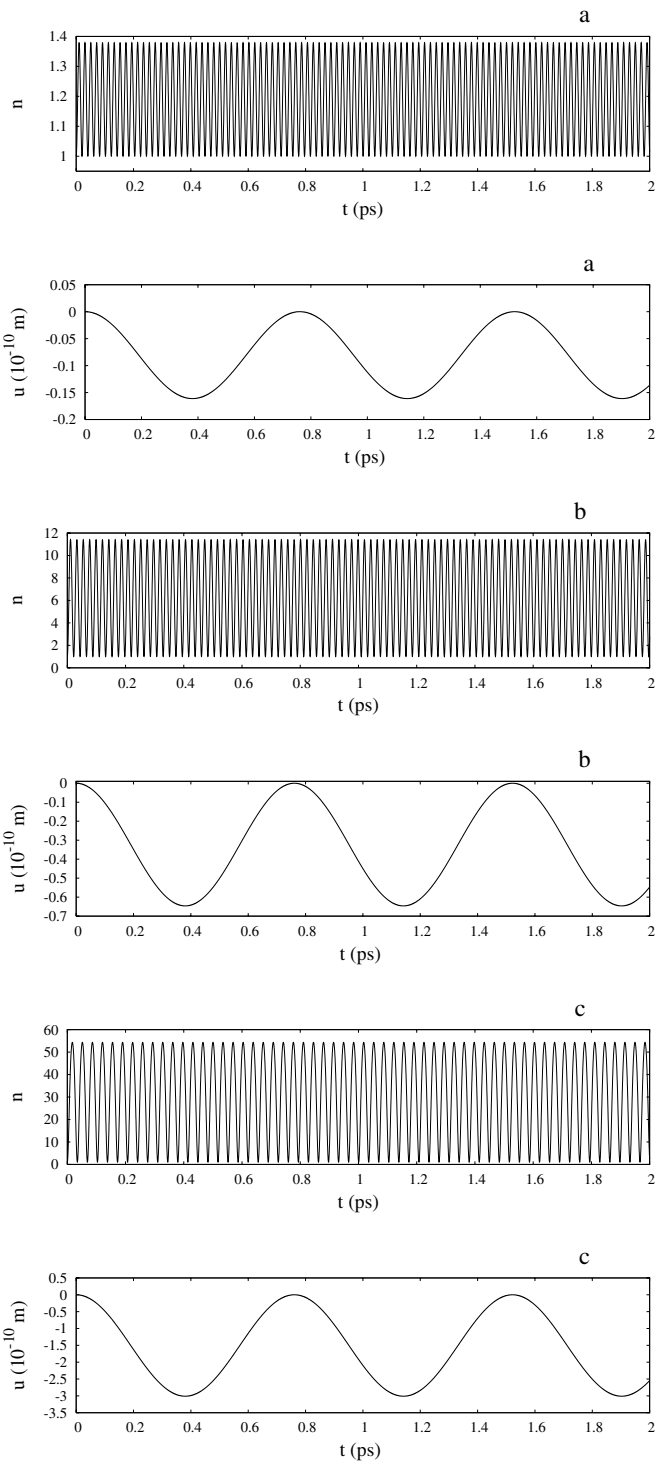

FIG. 7. Adiabatic results for the average number of excitations (n) and quasistatic results for the lattice distortion (u) with $T=10$ (a), 50 (b), and 90 (c) (in units of 10^{-21} J). The initial conditions are as in Fig. 1.

In the case $T=0$ the quartic polynomial has two double real roots: $n_1=1$ and $n_2=2(k\varepsilon_0/\chi^2-1)$. This case is, however, not relevant because the possibility $T=0$ was excluded in the derivation of Eq. (23) (see the Appendix). It would obviously correspond to the conservative Davydov monomer with a different set of equations of motion.

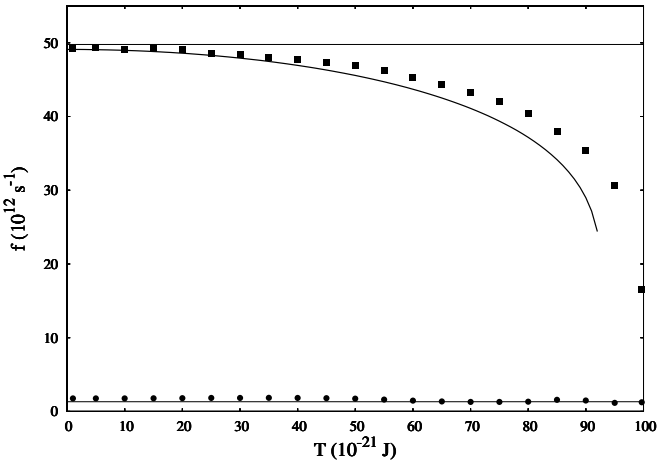

FIG. 8. Frequency of oscillation of the average number of excitations and lattice distortion as functions of T in the range $0<T<T_c$: average frequency of oscillation of the number of excitations determined numerically (squares); average frequency of oscillation of the lattice distortion determined numerically (circles). The thick line corresponds to the frequency of oscillation of the number of excitations predicted by the adiabatic approximation [Eq. (28)]. The horizontal thin lines correspond to $f=\varepsilon_0/2\pi\hbar\simeq 50$ and $f=(1/2\pi)\sqrt{k/M}\simeq 1$.

The characteristics of the solutions for the other cases are given below.

A. $0<T<T_c$

In this range the quartic polynomial has four distinct real roots $n_4>n_3>n_2>n_1=1$, which are functions of T (as well as of the parameters of the Hamiltonian). The solution of (25) is [16]

$$n(t) = \frac{(n_4-n_2)+n_4(n_2-1)\mathrm{sn}^2[\sqrt{(\alpha/8)(n_4-n_2)(n_3-1)}t,\mathrm{mod}]}{(n_4-n_2)+(n_2-1)\mathrm{sn}^2[\sqrt{(\alpha/8)(n_4-n_2)(n_3-1)}t,\mathrm{mod}]} \tag{26}$$

where

$$\mathrm{mod}^2=\frac{(n_4-n_3)(n_2-1)}{(n_4-n_2)(n_3-1)} \tag{27}$$

is the Jacobi modulus.

Equation (26) describes periodic solutions of (25) (see Fig. 7), which can be compared with the corresponding numerical ones (cf. Fig. 1).

It is apparent that the adiabatic approximation is able to reproduce the amplitude of $n(t)$, as well as the general trend of an increasing period of oscillation when T increases. The main difference between numerical (Fig. 1) and adiabatic (Fig. 7) results is the slow modulation displayed by the former, in both amplitude and frequency, which is a feature of the dynamics for all values of T. The adiabatic approximation cannot capture features that occur in slow time scales since this approximation is valid only in the opposite regime.

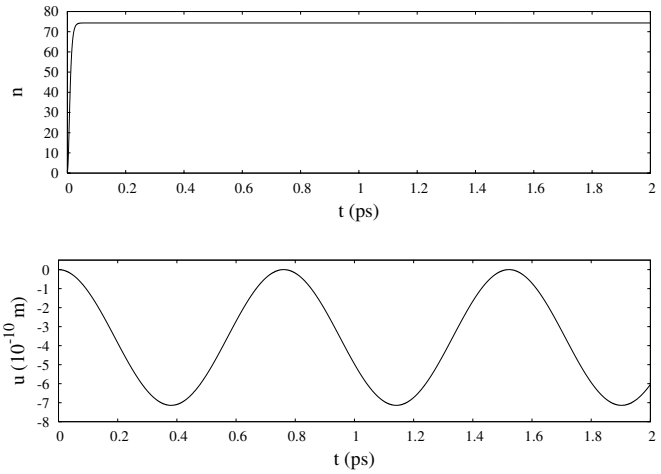

FIG. 9. Adiabatic results for the average number of excitations (n) and quasistatic results for the lattice distortion (u) with $T=T_c$. The initial conditions are as in Fig. 1.

The Fourier transforms associated with the numerical solutions (Fig. 2) illustrate their complexity. The approximate solutions have spectra showing essentially a single peak centered at a frequency which is given by

$$f = \frac{\sqrt{(\alpha/8)(n_4 - n_2)(n_3 - 1)}}{K(\mathrm{mod})}. \tag{28}$$

In Eq. (28) $K(\mathrm{mod})$ is the complete elliptic integral of the first kind corresponding to the modulus mod. Since the roots of the quartic polynomial present in Eq. (28) are functions of T, so is the single frequency of oscillation associated with the approximate solutions. In Fig. 8 the variation of the frequency with T is displayed and compared with the average frequency that was calculated from the numerical solutions. The latter is computed by weighting each frequency present in the corresponding spectrum with the associated relative power. Figure 8 shows a good correlation between the two curves.

B. $T=T_c$

If $T=T_c$, then the polynomial has four real roots, but two of them are equal. The single roots are $n_1=1$ and $n_3=8k\varepsilon_0/3\chi^2-3$ and the double one is $n_2=2k\varepsilon_0/3\chi^2$ ($n_3>n_2>n_1$). The solution of Eq. (25) has, in this case, the analytical form

$$n(t) = \frac{(8k\varepsilon_0/3\chi^2 - 3)\tanh^2[\sqrt{3}(\varepsilon_0/\hbar + \chi^2/2k\hbar)t] + 3}{\tanh^2[\sqrt{3}(\varepsilon_0/\hbar + \chi^2/2k\hbar)t] + 3} \tag{29}$$

Equation (29) corresponds to the limit of Eq. (26) when T approaches T_c. In this condition the Jacobi modulus given by Eq. (27) becomes equal to 1 and the Jacobi sn function becomes the tanh function [16]. This is not a periodic solution, in agreement with the infinite limit of the period of (26), given by Eq. (28) (see Figs. 8 and 9).

In the case $T=T_c$ there are no numerical solutions to compare with the adiabatic approximation because the exact T value that leads to the onset of the transition between the two observed regimes is not known.

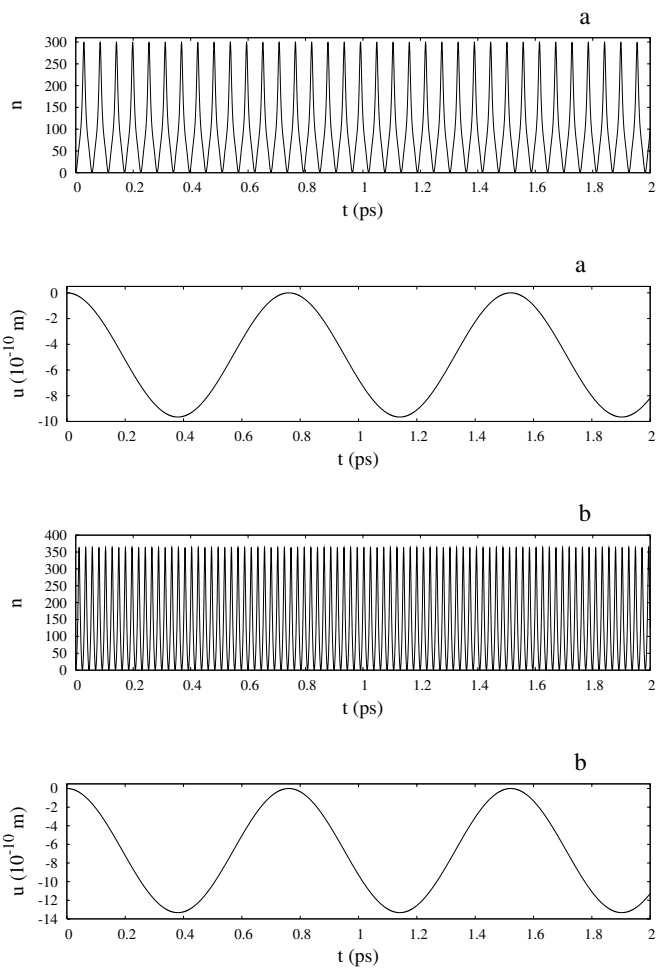

FIG. 10. Adiabatic results for the average number of excitations (n) and quasistatic results for the lattice distortion (u) with $T=100$ (a) and 200 (b) (in units of 10^{-21} J). The initial conditions are as in Fig. 1.

C. $T>T_c$

In this last case the quartic polynomial has two distinct real roots $n_2>n_1=1$; and two complex conjugate roots $n_r \pm i n_i$. The solutions obtained in the adiabatic approximation are [16]

$$n(t) = \frac{(A - n_2 B)\mathrm{cn}(\sqrt{(\alpha/2)AB}t, \mathrm{mod}) + (n_2 B + A)}{(A - B)\mathrm{cn}(\sqrt{(\alpha/2)AB}t, \mathrm{mod}) + (A + B)}, \tag{30}$$

where $A=\sqrt{(n_2-n_r)^2+n_i^2}$, $B=\sqrt{(1-n_r)^2+n_i^2}$, and

$$\mathrm{mod}^2 = \frac{(n_2 - 1)^2 - (A - B)^2}{4AB}. \tag{31}$$

The dependence of this solution on T is given through n_2, n_r, and n_i.

The periodic behavior of $n(t)$ is resumed above T_c with the period $\tau=4K(\mathrm{mod})/\sqrt{\frac{\alpha}{2}AB}$. Examples of this kind of so-

lution are plotted in Fig. 10. Comparison of this figure with Fig. 3(c) demonstrates the failure of the adiabatic approximation in this regime. Of course, a complete comparison between numerical and adiabatic solutions is not possible for these values of T since the numerical results are limited by the relative failure in the preservation of the conserved quantities, like the total energy.

As just seen above, in the adiabatic approximation the system shows a transition occurring for the critical value $T=T_c$. This value of the parameter separates two qualitatively different regimes of the system. A small increment of T over T_c produces a drastic increase in the amplitude of the oscillations. One should notice that, for the initial conditions considered, the total energy of the system is independent of T. The increment of T allows, therefore, for the creation of a large number of amide I excitations without increasing the total energy of the system.

The sudden change in the qualitative behavior of the excitation dynamics given by the adiabatic approximation is reminiscent of the observations made with the numerical solutions (Fig. 3). Indeed, while numerically a transition occurs at $T_c \simeq 99.7$ $(10^{-21}$ J), the approximate value, obtained from Eq. (25), is $T_c=\sqrt{(2k/3^3\chi^2)(\varepsilon_0-3\chi^2/2k)^3} \simeq 92.9$ $(10^{-21}$ J). Equation (25) is thus capable of predicting a transition with 93% accuracy, thus providing further confirmation of the numerical results.

On the other hand, the behavior described by the adiabatic approximation above the transition is different from the numerical one. In fact, while the approximate dynamics is periodic, the numerical dynamics expands to an increasing number of excitations, as time increases.

Let us now address the lattice dynamics.

From Eqs. (20) and (21), the differential equation for the distortion is

$$\ddot{u}(t) = -\frac{\chi}{M}\left(n(t)+\frac{1}{2}\right) - \frac{k}{M}u(t). \tag{32}$$

Since, as stated above, the lattice is expected to evolve more slowly than the excitations, it will be assumed in Eq. (32) that the former responds only to the time average of the latter: the quasistatic approximation. Equation (32) is therefore simplified to

$$\ddot{u}(t) + \frac{k}{M}u(t) = -\frac{\chi}{M}\left(\bar{n}+\frac{1}{2}\right), \tag{33}$$

where $\bar{n}$ is the (constant) time average of $n(t)$. Equation (33) is the equation of an oscillator driven by a constant force. For the initial conditions used before ($u_0=0\times10^{-10}$ m and $p_0=0\times10^{-23}$ kg m s^{-1}), the solution of Eq. (33) is

$$u(t) = \frac{\chi}{k}\left(\bar{n}+\frac{1}{2}\right)\left[\cos\left(\sqrt{\frac{k}{M}}t\right)-1\right]. \tag{34}$$

The dependence of $u(t)$ on the parameter T is indirectly given through $\bar{n}$. Some examples of the solutions for the lattice distortion are displayed in Figs. 7, 9, and 10.

The curves change continuously with T except near T_c. The shape of $u(t)$ is generally the same below and above that value, corresponding to the same kind of dynamics. In both regions the amplitude and the mean level of the oscillations show a smooth dependence on T. In fact, the abrupt jump observed for $T=T_c$ is an indirect consequence of the transition occurring in $\bar{n}$ (cf. Figs. 7 and 10).

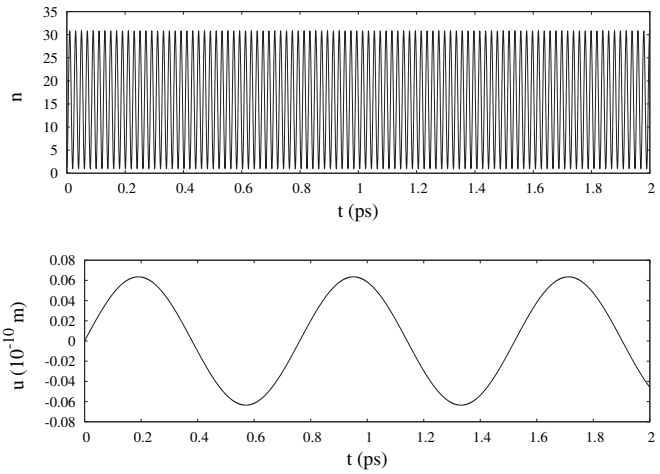

FIG. 11. Average number of excitations and lattice distortion for $T=90$ (in units of 10^{-21} J). Initial conditions are $\xi_{r0}=\xi_{i0}=0$, $u_0=0$ $(10^{-10}$ m), $p_0=1$ $(10^{-23}$ kg m s^{-1}), and $n_0=1$. The interaction parameter χ was set to zero in this simulation.

For small values of T ($T\leqslant 25$), the behavior displayed by the lattice in the quasistatic approximation is similar to that predicted by the numerical solutions. This fact can be appreciated by comparing Figs. 1 and 7, particularly plots (a). A difference becomes apparent, in quantitative terms, as T is increased. The general trend is that the amplitude and the level of the lattice distortion increase more slowly with T in the numerical solution (see plots in Figs. 1 and 7). The numerical solutions also display a small variation in the average frequency of the lattice oscillation which is not reproduced by the quasistatic results. This feature can be seen in Fig. 2 which shows that the Fourier transforms of $u(t)$ have peaks whose positions shift for different values of T and is also apparent in Fig. 8 where the frequencies of the numerical solutions (circles) are compared with the frequency predicted by the quasistatic approximation, namely, $f=(1/2\pi)\sqrt{k/M}$.

Finally, as discussed above, the cases $T=99.69$ and $T=99.7$ are out of the range of validity of the quasistatic approximation (see plots in Figs. 3 and 10).

V. CONCLUDING REMARKS

The Hamiltonian (9) describes the interaction between two oscillators. The vibrational excited states (excitations) of a carbonyl group (which can arise in polypeptide chains) are coupled to the distortions of an adjacent hydrogen bond. In addition to that interaction, a term that does not conserve the excitation was also included in Hamiltonian (9). The role of this term is to allow for the possible decay of the energy stored in the amide I vibrations and the use of this energy to promote conformational changes. The strength of this nonconserving term is given by the parameter T. The hypothesis

in the present study is that storing of amide I vibrations is a step in the mechanism of protein function and that the conformational changes associated with protein work are due to the release of this energy to the classical degrees of freedom of the protein.

In this work, the equations of motion derived from (9) were numerically integrated. The results obtained are consistent with the conclusion that the nonconserving term drives a fast oscillation of the average excitation number with the frequency $f=\varepsilon_0/2\pi\hbar$. Its amplitude is an increasing function of T. These would be, in fact, the observed characteristics of the function $n(t)$ if the parameter χ was set to zero in Eqs. (17)–(21).

Due to the presence of the interaction term, the fast oscillation of the average number of excitations induces the movement of the lattice by originating a "force" essentially related to the time average of $n(t)$ $(\bar{n})$. The effect of this force is mainly to displace the equilibrium position of the lattice, that is, to change the average length of the associated hydrogen bond. The resulting lattice distortion is an oscillation around the new equilibrium position $\bar{u}=-(\chi/k)(\bar{n}+1/2)$, dependent on the initial conditions and with the natural frequency of the lattice: $(1/2\pi)\sqrt{k/M}$. The motion of the lattice is, in turn, responsible for the modulations in both the amplitude of $n(t)$ and its frequency.

These conclusions are apparent when we compare Figs. 1 and 11. For the simulation displayed in Fig. 11, the interaction parameter was set to zero ($\chi=0$). In these conditions the variation of the average number of excitations is decoupled from the movement of the lattice. Both subsystems evolve independently of each other. Comparing Figs. 1 and 11 one may easily conclude that the effect of the interaction term is indeed the modulation of the regular, fast, oscillation of the average number of excitations (in amplitude and frequency), as well as the contraction of the lattice. This contraction is already observed in the Davydov-Scott model, which does not include the nonconservative term. The displacement of the equilibrium position of the lattice consequently enhances its amplitude of oscillation.

The dynamics of the total system is strongly dependent on T. As T increases, the amplitude of $n(t)$ increases—following a polynomial law of third degree in T, which is to be compared with the parabolic law that would be obtained by setting χ to zero in the equations of motion (17)–(21), thus inducing a stronger oscillation of the lattice. As a consequence, $n(t)$ is further deformed by the modulations in amplitude and frequency. A small variation of the lattice oscillation frequency is also observed for different T values.

An important characteristic of this system is that, for a specific value of the parameter T (T_c), there occurs a transition in the qualitative behavior of the dynamics. A critical value of $\simeq 99.7$ $(10^{-21}$ J) was determined from numerical simulations. For values of T above T_c the dynamics of the system becomes very complex suggesting the onset of chaotic behavior in the system. This question was not addressed in the present paper but requires further investigation.

Some results not shown in this paper suggest that the critical value, T_c, depends on the energy of the system. The value given above is obtained when the total energy of the system is $E=1.5\varepsilon_0$.

The transition described seems to be related to the onset of a resonance between the oscillation of the average number of excitations and of the lattice displacement. Indeed, Fig. 8 shows that the average frequency associated with $n(t)$ decreases monotonically with increasing T. As T approaches T_c, the average frequency becomes closer to the frequency of the lattice oscillation. More work is needed for a complete mathematical understanding of this feature.

The simulations show that there is not a strong dependence of the behavior of the system on the initial conditions (see Figs. 4 and 5). Nevertheless, apart from slightly different time evolutions, which are expected when the system is started at different points, another feature was observed. In fact, varying the phase of the initial complex parameter $\xi=\langle\psi(0)|\hat{a}|\psi(0)\rangle$ induces different time evolutions for the observables of the system. Although this is not a common result, it has been reported before [14].

The adiabatic approximation performed on Eqs. (17)–(21) led to a nonlinear differential equation for the average number of excitations in the system (25). The solutions of this equation have been found for the different regimes determined by T and for a fixed set of initial conditions. The study of the quartic polynomial [right-hand side of Eq. (25)] allows by itself the establishment of a critical value of T separating qualitatively different solutions of the equation. This is an important result because it allows us to discard the possibility of artifacts in the numerical integration of the equations of motion. The fact that in the adiabatic approximation a transition is still observed is in support of the real existence of such a transition in the system. The comparison between the critical value of T obtained in this approximation and the numerically obtained one is good. The relative difference between them is $\simeq 7\%$.

The study of the polynomial on the right-hand side of Eq. (25) also allows us to predict that the dynamics of the system is not sensitive to the sign of T. This result is as observed in the numerical solutions.

One should notice that the exact value of T_c for the system is not known. The value of $\simeq 99.7$ mentioned above is obtained by systematically increasing the parameter T in Eqs. (17)–(21), solving them numerically, and checking afterward whether the solutions have qualitatively changed or not. For this reason it is only possible to state that $99.69 < T_c < 99.70$. A comparison between the behavior of the adiabatic solution for $T=T_c$ [Eq. (29)] and the corresponding numerical one is therefore impossible. Moreover, for high values of T $(T>99.7)$ it was not possible to determine numerical solutions while keeping constant the quantities theoretically expected to be conserved (although only variations in the last three or four of nine significant digits were observed). Comparison of these results with the adiabatic predictions are therefore only performed for short-time dynamics. By comparing Figs. 3(c) and 10 one may readily conclude that the adiabatic approximation is not able to give good results in this T domain. In fact, while the adiabatic result for $n(t)$ consists of an oscillation with well-defined values of both the frequency and the

amplitude, the behavior of the numerical solution is clearly more complex.

The comparison between numerical and adiabatic solutions must therefore be established for the values of T below T_c. The general observed trend is that the approximation is fairly good for small values of T and gets worse as T approaches T_c. The approximation makes good predictions for the maximum amplitude of $n(t)$ but not for its modulation. As a consequence, the approximation gets worse as the modulation gets stronger (with increasing T). The adiabatic approximation is not able to predict the modulation of $n(t)$ in frequency, a feature that is observed even for small values of T in the numerical solutions. In spite of this fact, the frequency predicted by the approximation shows the same trend as the average frequency displayed by the numerical solutions (cf. Fig. 8). The decrease of the frequency, observed in both numerical and adiabatic solutions, is the reason why the approximation fails when T approaches T_c. Indeed, the approximation is based on the assumption that two distinct time scales exist for the dynamics of the excitations and of the lattice. It is apparent in Fig. 8 that this assumption does not hold true when T is increased.

Concerning the lattice motion, the general trend mentioned is valid, i.e., for small values of T ($T \leqslant 25$) there is a good agreement between the distortion computed numerically and the quasistatic results. Also, the main feature that the contraction of the lattice is enhanced when the average number of excitations rises is predicted. Moreover, as T approaches the critical value, the approximation is still capable of predicting the qualitative behavior of $u(t)$ but with pronounced differences in the amplitude and less pronounced differences in the frequency of the oscillation.

The model presented in this paper describes essentially a contraction of a hydrogen bond when the adjacent carbonyl group is in an excited state. Unlike the case of the one-site Davydov-Scott model, this contraction is time dependent because the number of amide I excitations is not conserved. Due to the presence of amide I excitations, the lattice oscillates around a contracted equilibrium position. If we take the time average of the number of excitations and of the lattice distortion, the results reported here tend to what is found for the Davydov-Scott model: $\bar{u} = -(\chi/k)(\bar{n} + 1/2)$.

Only one excitable site was considered in this paper. The model should be generalized in order to include more sites for amide I excitations. This will lead to a more complex local dynamics since a second channel for energy transfer becomes available. In the general case, we can foresee that the presence of amide I excitations at one site will induce oscillations of the adjacent hydrogen bond until some of the excitations are transferred to another site, leading to the propagation of the lattice oscillations to the entire structure. One can picture an α helix undergoing local contractions as amide I excitations are created and transferred along it.

It should be kept in mind that, for specific values of the nonconservative parameter T, the system exhibits completely different dynamics. In those cases the hydrogen bond is forced to physically impossible contractions. This is due to the fact that the lattice potential considered is harmonic. Its substitution by a more realistic potential should prevent that feature. A realistic potential should also account for the possibility of hydrogen bond breaking, something that is not possible with the harmonic potential. With these considerations, and remembering that the values of the parameters of the Hamiltonian are not completely known, those values of T may still prove to be physically relevant. In fact, the sign of the interaction parameter χ determines whether the lattice is contracted or expanded. A negative χ leads to a strong expansion (eventually to the breaking) of the hydrogen bond when combined with a high value of T and a realistic potencial. Recent work suggests the possibility of a negative χ, instead of the positive value that has traditionally been used [17].

The motivation for this work is to develop a model that can explain protein conformational changes. For these to occur, some of the hydrogen bonds that stabilize a given conformation must be broken and different ones must be formed. The hypothesis here is that the energy for these processes comes from the decay of vibrational excited states. The Hamiltonian explored here did show changes in the hydrogen bonds, but more in the direction of strengthening the hydrogen bonds than weakening them. As explained above, a Lennard-Jones potential for the lattice, together with a negative nonlinearity parameter, should lead to bond breaking. Thus, the overall conclusion is that, although some questions remain to be explored, the type of Hamiltonian studied here does provide a mechanism for protein function.

ACKNOWLEDGMENT

The Fundação para a Ciência e a Tecnologia is acknowledged for financial support to P.A.S.S.

APPENDIX

In this appendix Eq. (23) is derived from Eqs. (17)–(21) and the condition (22).

Taking the time derivative of (17) and using (19), one finds

$$\ddot{n}(t) = \frac{2T}{\hbar^2}[\varepsilon_0 + \chi u(t)]\xi_r(t) + \frac{2T^2}{\hbar^2}. \tag{A1}$$

On the other hand, from Eqs. (17) and (18) we have

$$\dot{\xi}_r(t) = -\frac{\varepsilon_0 + \chi u(t)}{2T}\dot{n}(t), \tag{A2}$$

where it was assumed $T \neq 0$. As mentioned above, T in Eqs. (17)–(21) is an unknown parameter related to the rate of variation of the number of excitations. In the case $T=0$, that number would be conserved and the resulting equations of motion would have an exact solution.

From condition (22) and Eq. (21) one can write $u(t) \approx -(\chi/k)[n(t) + 1/2]$, which, when inserted in Eqs. (A1) and (A2) leads to

$$\ddot{n}(t) = \frac{2T}{\hbar^2}\left[\varepsilon_0 - \frac{\chi^2}{k}\left(n(t) + \frac{1}{2}\right)\right]\xi_r(t) + \frac{2T^2}{\hbar^2}, \tag{A3}$$

$$\dot{\xi}_r(t) = \left[-\frac{\varepsilon_0}{2T} + \frac{\chi^2}{2Tk}\left(n(t) + \frac{1}{2}\right)\right]\dot{n}(t). \tag{A4}$$

Equation (A4) can be integrated to the form

$$\xi_r(t) = \frac{\chi^2}{4Tk}n^2(t) - \left(\frac{\varepsilon_0}{2T} - \frac{\chi^2}{4Tk}\right)n(t) - \frac{\chi^2 n_0^2}{4Tk} + \left(\frac{\varepsilon_0}{2T} - \frac{\chi^2}{4Tk}\right)n_0 + \xi_{r0}, \tag{A5}$$

where n_0 and ξ_{r0} are the initial values of $n(t)$ and $\xi_r(t)$. Inserting this equation in (A3) one obtains an equation involving only the function $n(t)$ [Eq. (23)]:

$$\ddot{n}(t) = -\alpha n^3(t) + \beta n^2(t) - \gamma(n_0, \xi_{r0})n(t) + \delta(n_0, \xi_{r0}) + \frac{2T^2}{\hbar^2}.$$

The parameters in this equation are $\alpha = \chi^4/2k^2\hbar^2$, $\beta = (3\chi^2/2k\hbar^2)(\varepsilon_0 - \chi^2/2k)$,

$$\gamma(n_0, \xi_{r0}) = \frac{(\varepsilon_0 - \chi^2/2k)^2}{\hbar^2}\left[1 - \frac{1}{2}\left(\frac{\chi^2}{k(\varepsilon_0 - \chi^2/2k)}\right)^2 n_0^2 + \frac{\chi^2}{k(\varepsilon_0 - \chi^2/2k)}n_0 + 2\frac{\chi^2}{k(\varepsilon_0 - \chi^2/2k)}\frac{T}{(\varepsilon_0 - \chi^2/2k)}\xi_{r0}\right],$$

and

$$\delta(n_0, \xi_{r0}) = \frac{(\varepsilon_0 - \chi^2/2k)^2}{\hbar^2}\left(-\frac{1}{2}\frac{\chi^2}{k(\varepsilon_0 - \chi^2/2k)}n_0^2 + n_0 + 2\frac{T}{(\varepsilon_0 - \chi^2/2k)}\xi_{r0}\right).$$

[1] C. W. F. McClare, Ann. N.Y. Acad. Sci. **227**, 74 (1974).
[2] A. S. Davydov, J. Theor. Biol. **38**, 559 (1973).
[3] A. S. Davydov, *Biology and Quantum Mechanics* (Pergamon, Oxford, 1982).
[4] A. Scott, Phys. Rep. **217**, 1 (1992), and references therein.
[5] L. Cruzeiro-Hansson and S. Takeno, Phys. Rev. E **56**, 894 (1997).
[6] G. Careri, U. Buontempo, F. Galluzzi, A. C. Scott, E. Gratton, and E. Shyamsunder, Phys. Rev. B **30**, 4689 (1984).
[7] J. Edler and P. Hamm, J. Chem. Phys. **117**, 2415 (2002).
[8] J. Edler and P. Hamm, J. Chem. Phys. **119**, 2709 (2003).
[9] J. Edler and P. Hamm, Phys. Rev. B **69**, 214301 (2004).
[10] R. H. Austin, A. Xie, L. Meer, M. Shinn, and G. Neil, J. Phys.: Condens. Matter **15**, S1693 (2003).
[11] L. Cruzeiro-Hansson and P. A. S. Silva, J. Biol. Phys. **27**, S6 (2001).
[12] P. A. S. Silva and L. Cruzeiro-Hansson, Phys. Lett. A **315**, 447 (2003).
[13] L. Cruzeiro-Hansson and V. M. Kenkre, Phys. Lett. A **203**, 362 (1995).
[14] V. M. Kenkre and H.-L. Wu, Phys. Lett. A **135**, 120 (1987).
[15] J. A. Tuszynski, M. L. A. Nip, P. L. Christiansen, M. Rose, and O. Bang, Phys. Scr. **51**, 423 (1995), and references therein.
[16] P. F. Byrd and M. D. Friedman, *Handbook of Elliptic Integrals for Engineers and Physicists* (Springer-Verlag, Berlin, 1954).
[17] L. Cruzeiro, J. Chem. Phys. **123**, 234909 (2005).